Carbohydrate Polymers 84 (2011) 1033–1038

Contents lists available at ScienceDirect

Carbohydrate Polymers

journal homepage: www.elsevier.com/locate/carbpol

A comparative study of *Eucalyptus* and *Pinus radiata* pulp fibres as raw materials for production of cellulose nanofibrils

Kristin Syverud [a,*], Gary Chinga-Carrasco [a], Juan Toledo [b], Pedro G. Toledo [b]

[a] *Paper and Fibre Research Institute, PFI, Høgskoleringen 6b, 7491 Trondheim, Norway*
[b] *Department of Chemical Engineering, Universidad de Concepción, Concepción, Chile*

ARTICLE INFO

Article history:
Received 6 September 2010
Received in revised form 1 December 2010
Accepted 21 December 2010
Available online 30 December 2010

Keywords:
Microfibrillated cellulose (MFC)
Computerized image analysis
Microscopy
Metrology
Nanotechnology

ABSTRACT

This work comprises a comparison between *Eucalyptus* and *Pinus radiata* pulp fibres, as raw materials for producing nanofibrils. The cellulose nanofibrils were produced mechanically and chemi-mechanically. Series of the fibres were subjected to a TEMPO mediated oxidation to facilitate the homogenization. The contents of carboxyl acids after the pre-treatment indicated a favourable situation for producing nanofibrils using *Eucalyptus* pulp fibres as raw material. However, films made of *P. radiata*-based nanofibrils evidenced less shrinkage and higher transparency levels, which were related to a higher fibrillation of the pulp fibres. The energy consumption during homogenization was quantified. The results demonstrated that for a given number of passes through the homogenizator, TEMPO pre-treatment will facilitate the homogeneous fibrillation of a given fibre. This implies that less energy is required for producing nanofibrils with homogeneous sizes.

1. Introduction

1.1. Cellulose nanofibrils

Cellulose nanofibrils are produced through a fibrillation of cellulose fibres (Turbak, Snyder, & Sandberg, 1983). Nanofibrils have diameters of roughly less than 100 nm, lengths of several micrometers and have thus a large aspect ratio. In addition, nanofibrils are highly crystalline, which provides extremely high mechanical properties. Having a large aspect ratio, a large specific surface area with reactive OH-groups proposes the nanofibrils as an interesting material for several applications.

Since its introduction, a series of application areas have been suggested for the nanofibrillated material, e.g. for rheology adjustment and emulsion stabilizer of food, paint and cosmetics (Turbak, Snyder, & Sandberg, 1982, 1985). Recently, applications as strength enhancer in paper and composite materials have been explored (e.g. Eriksen, Syverud, & Gregersen, 2008; Henriksson & Berglund, 2007; Syverud & Stenius, 2009; Mörseburg & Chinga-Carrasco, 2009; Taniguchi & Okamura, 1998). Cellulose nanofibrils seem to be most adequate for barrier applications in novel packaging concepts (Aulin, Gällstedt, & Lindström, 2010; Hult, Iotti, & Lenes, 2010; Minelli et al., 2010; Syverud & Stenius, 2009). In addition, novel applications have been foreseen within medicine, where cellulose nanofibrils may e.g. be applied as scaffolds for tissue or bone (see e.g. review by Klemm et al., 2006).

Much research has been performed during the last years for releasing the nanofibrils from cellulose fibres in order to exploit their inherent properties. Several approaches have been demonstrated, including mechanical (Eriksen et al., 2008; Turbak et al., 1983; Zimmermann, Bordeanu, & Strub, 2010), enzymatic (Pääkkö et al., 2007) and chemical pre-treatments (Heijnes-Son-Hultén, 2007). With respect to chemical pre-treatments, TEMPO mediated oxidation has been applied for facilitating the fibrillation of pulp fibres (Saito, Nishiyama, Putaux, Vignon, & Isogai, 2006). TEMPO pre-treatment introduces carboxylic acid groups in the C6 position of the glucose unit, which also may be utilized for surface modification purposes (Syverud et al., 2010). Small amounts of aldehyde groups are also introduced by the TEMPO pre-treatment. However, according to Saito, Kimura, Nishiyama, and Iasogai (2007), the aldehyde groups have no influence on the cellulose nanofibril preparation.

1.2. Purpose of the study

Only a few studies have reported some results with respect to nanofibril production based on hard- and softwood pulp fibres (Fukuzumi, Saito, Iwata, Kumamoto, & Isogai, 2009; Stelte & Sanadi, 2009; Zimmermann et al., 2010). Hence, a detailed and direct comparison between pulp fibres from industrially farmed tree species such as *Eucalyptus* and *Pinus radiata* is most interesting. The purpose of the present study was thus to compare the suitability of

* Corresponding author. Tel.: +47 95903740; fax: +47 73550999.
E-mail address: kristin.syverud@pfi.no (K. Syverud).

0144-8617/$ – see front matter © 2010 Elsevier Ltd. All rights reserved.
doi:10.1016/j.carbpol.2010.12.066

Eucalyptus and *Pinus radiata* pulp fibres for producing nanofibrils. The effect of fibre type, pre-treatment with TEMPO mediated oxidation and homogenization on properties of the produced fibrils and films was quantified. The energy applied to produce a given nanofibril morphology was compared, which is most interesting from an industrial point of view.

2. Experimental

2.1. Fibre samples

Two never-dried market fully bleached kraft pulps were applied in this study. One of the pulps was an *Eucalyptus* pulp composed of 70% *Eucalyptus nitens* and 30% *Eucalyptus globulus*. The second pulp was composed of 100% *Pinus Radiata* fibres. None of the pulps were beaten.

2.2. Fibre chemical composition

The carbohydrate composition was determined before and after TEMPO-mediated oxidation, by using the TAPPI test method T 249 cm-85, modified according to Cao, Tschirner, Ramaswamy, and Webb (1997).

2.3. Production of nanofibrils

Series of the pulp fibres were chemically pre-treated. TEMPO mediated oxidation was thus performed according to Saito et al. (2006) where the 2,2,6,6-tetramethylpiperidinyl-1-oxyl (TEMPO) radical catalyzes oxidation of primary alcohol groups using NaClO. 0.025 g TEMPO and 0.25 g NaBr was dissolved in 150 ml distilled water. 2 g of the cellulose pulp calculated as dry matter content and 12.3 mmol anhydroglucose unit (AGU, $C_6H_{10}O_5$), was suspended in the solution. NaClO (3.8 mmol) was added per gram cellulose pulp giving 0.6 in the molar ratio $NaClO/C_6H_{10}O_5$. According to Saito et al. (2006) the most efficient fibrillation of the fibres was obtained after oxidation with the mentioned molar ratio. The pH was kept constant at 10.5 by adding NaOH. The reaction time was approximately 30 min and was performed at room temperature. The reaction was finished when there were no longer changes in pH. The pH was then adjusted to 7 by addition of HCl and the pulp was washed with distilled water at room temperature on a Büchner funnel with filter cloth (140 mesh). The amount of charged groups (glucuronic acids) was measured by potentiometric titration. Two replicates were undertaken for each sample.

The oxidized fibres were then homogenized with a Rannie 15 type 12.56× homogenizer operated at 1000 bar pressure. The pulp consistency during homogenization was 0.5%. This is a very low concentration that leads to high energy consumption, but was chosen in order to avoid runnability problems with homogenization of non-pre-treated softwood fibres. For comparison purposes, the same concentration was applied in the trials. In addition, two series were homogenized directly without the TEMPO pre-treatment. Samples of fibrils were collected after 3 and 5 passes through the homogeniser. Energy consumption during the homogenization was measured using an effect reader, a NI USB-6009 a/d converter and a computer running the LabView software. The production of nanofibrils and the subsequent film manufacturing were performed according to a 2^4 factorial experiment, as described in Table 1. In addition two series of the oxidized *P. Radiata* pulp fibres were homogenized at 200 and 600 bar for verifying the energy consumption and corresponding nanofibril production at lower pressure. Nanofibrils were collected after 1, 3 and 5 passes for comparison purposes.

Table 1
Runs applied for preparing the nanofibril-based films. The series were made randomly according to the sequence specified in the run order column. The "*" indicates that the films F01–F08 were additionally made with a temperature of 30 °C. The applied variables were Fibre (E: *Eucalyptus* and R: *Pinus Radiata*), pre-treatment (0: no pre-treatment and T: TEMPO mediated oxidation), homogenization (3 and 5 pass), drying (23 and 30 °C).

Series	Run order	Fibre	Pre-treatment	Homogenization (# pass)	Drying (°C)
F01	2	E	0	3	23
F02	9	R	0	3	23
F03	14	E	T	3	23
F04	12	R	T	3	23
F05	1	E	0	5	23
F06	13	R	0	5	23
F07	3	E	T	5	23
F08	16	R	T	5	23
F01*	8	E	0	3	30
F02*	5	R	0	3	30
F03*	10	E	T	3	30
F04*	7	R	T	3	30
F05*	11	E	0	5	30
F06*	15	R	0	5	30
F07*	6	E	T	5	30
F08*	4	R	T	5	30

2.4. Degree of polymerization

The degree of polymerization (DP) was estimated according to Sihtola, Kyrklund, Laamanen, and Palenius (1963). The intrinsic viscosity data was obtained following a standard method (ISO 5351).

2.5. Preparation of films

Ten films (20 g/m^2) were made for each series. The films were prepared by placing a given amount of the suspensions in a plastic Petri dish. The films were allowed to dry at 23 °C and at 30 °C. In total 16 series of films were made according to Table 1. The nanofibril production and film preparation were performed randomly.

2.6. Film characteristics

After free drying, the films were released carefully from the Petri dishes. The tensile index was measured according to ISO 1924-2:1994. Six replicates were used for these measurements. The tensile index was measured with a Zwick material tester (T1-FRxxMOD.A1K, serial no. 119249, model 2005). Conditions in the test room were: relative humidity 50%, temperature 23 °C. Four randomly chosen films from each series were placed on an Epson Perfection 4990 scanner and images were acquired in transmission mode at 300 DPI resolution. A shrinkage factor was quantified as the fraction between the projected area of the films and the circular area of the Petri dishes. In addition, approximately 1.5 cm × 8 cm strips were cut from the films. Some strips were placed on the scanner and covered with a glass plate for flattening the samples. Images were acquired at 2400 DPI in transmission mode. An IT8 calibration target (LaserSoft Imaging, Inc., Germany) was applied during acquisition in transmission mode for verification of the scanner stability. The transparency values were quantified as the fraction between the greylevel of the films and the greylevel of the background. The applicability of desktop scanners for assessing the transparency levels of films is introduced in this study. In addition, it is worth to mention that desktop scanners have been applied for quantification of some paper and film characteristics, which confirms the suitability and adequacy of such devices for scientific purposes (Chinga-Carrasco & Syverud, 2010; Dexter, 1993).

Atomic force microscopy (AFM, Nanoscope Dimension 3100 controller, Digital Instruments, VECCO-USA) was applied for sur-

Table 2
Relative carbohydrate composition of *Eucalyptus* and *Pinus radiata* pulp fibres. For comparison purposes, the measurements have been performed before and after TEMPO mediated oxidation.

Fibre component	*Eucalyptus* (%)		*Pinus radiata* (%)	
	Before	After	Before	After
Arabinose	0.3	0.3	1.1	0.3
Xylose	20.3	21.4	8.6	9.2
Mannose	0.2	0.2	5.3	2.7
Galactose	0.2	0	0.3	0
Glucose	79.0	78.1	84.9	87.8
Sum polysaccharides	100	100	100	100

face assessment at the nanoscale. The AFM analysis was performed on local areas of 5 μm × 5 μm, with a lateral resolution of 10 nm. The surface roughness (Sq) at several wavelengths was assessed with the SurfCharJ plugin, as described by Chinga, Johnsen, Dougherty, Lunden-Berli, and Walter (2007).

3. Results and discussion

3.1. Chemical analysis

The carbohydrate composition of the pulp fibres was assessed before and after TEMPO-mediated oxidation (Table 2). As expected, the results indicate a notorious difference between the *Eucalyptus* and *Pinus radiata* pulp fibres. The *Eucalyptus* has a larger fraction of xylose and less glucose compared to the *Pinus radiata*. The xylose content is not significantly affected by the TEMPO-mediated oxidation. *Eucalyptus* contains thus more hemicelluloses than *Pinus radiata*. It has been reported that high content of hemicelluloses facilitates the release of nanofibrils during the mechanical treatment of the pulp (Iwamoto, Abe, & Yano, 2008).

In addition to the carbohydrate composition, the carboxyl acid content after the TEMPO mediated oxidation was quantified. The amount of charged groups per unit mass was quantified to be 0.74 (std = 0.01) and 0.50 (std = 0.01) mmol/g for *Eucalyptus* and *P. Radiata*, respectively. In addition, the molar ratio of NaOCl/AGU was 0.6 giving DS of 13% for *Eucalyptus* and 8% for *P. Radiata*. The results are in good agreement with Habibi, Chanzy, and Vignon (2006), who reported a degree of substitution (DS) of 9.7% of whiskers after oxidation with a molar ratio of NaOCl/AGU of 0.5. The reaction conditions were the same for the two pulps, but still the DS was different. This was probably due to differences in the carbohydrate composition. The *Eucalyptus* pulp had higher content of hemicelluloses than the *P. radiata* pulp. Saito et al. (2006) reported the content of glucuronic acids to be 1.23 using the same reaction conditions on a never-dried sulphite pulp. However, the carbohydrate composition of this pulp was not reported. Contrary to xylose, mannose has also C6 primary hydroxyls, which may have been oxidized and dissolved out from the solid oxidized pulps. This may explain a minor part of the differences between the two pulps with respect to the amount of charged groups. The oxidation of pulp fibres has also been claimed to facilitate the release of nanofibrils (Saito et al., 2006). Hence, the contents of hemicelluloses and carboxyl acids after TEMPO mediated oxidation treatment indicate a favourable situation for producing nanofibrils, using *Eucalyptus* pulp fibres as raw material. This will be investigated in the following sections.

3.2. Degree of polymerisation

Table 3 gives the estimated DP of the cellulose pulp fibres and nanofibrils. The results indicate that there are slight differences between the two applied pulp fibres. The DP is consequently higher for *Eucalyptus* pulp fibres and the corresponding nanofibrils, compared to the *P. Radiata* materials. As reported by Saito and Isogai (2004), TEMPO mediated oxidation leads to a considerable reduction of the DP, when the oxidation is performed under alkaline conditions. In addition, the results in this study also indicate that even the homogenization of the pulp fibres reduces the DP. However, it is worth to mention that the viscosity of the TEMPO-mediated oxidised fibrils was outside the limits of the applied method.

Table 3
Viscosity data and degree of polymerization (DP) of cellulose pulp fibres and the corresponding cellulose nanofibrils produced after 5 pass through the homogenisator.

	Intrinsic viscocity (ml/g)		DP	
	Eucalyptus	*P. Radiata*	*Eucalyptus*	*P. Radiata*
Pulp fibres	890	880	1321	1305
Nanofibrils	670	650	965	934
TEMPO nanofibrils	140	120	171	144

3.3. Characteristics of the nanofibril-based films

Films were prepared in order to verify the effect of (i) the raw material, (ii) the pre-treatment, (iii) the homogenization and (iv) the drying, on the mechanical properties, shrinkage and transparency of the produced material.

The tensile index of films produced from *Eucalyptus* and *P. Radiata* nanofibrils are presented in Fig. 1. Note that the films F01 and F05, which were made of *Eucalyptus*-based nanofibrils have higher tensile index, than the corresponding *P. Radiata*-based nanofibrils. There is no significant difference between the corresponding films dried at the two applied temperatures. The results are in agreement with the corresponding DP-values (Table 3). It is worth to mention that the films made of TEMPO-mediated oxidized nanofibrils were brittle. Hence, it was not possible to properly measure the tensile index of films F03, F04, F07 and F08.

After drying, the films showed different degrees of shrinkage (Figs. 2 and 3, left). The quantification revealed that the fibrils produced from the *Eucalyptus* pulp fibres caused a larger shrinkage, compared to the *Pinus radiata*-based fibrils. In addition, increasing the number of passes and applying TEMPO pre-treatment reduced the shrinkage degree (Fig. 2). Contrary to the drying temperature effect, the fibre type, the TEMPO pre-treatment and the homogenization effects were significant. The films dried at 30 °C had a larger variation than the films dried at room temperature, even though the differences are still significant between the different

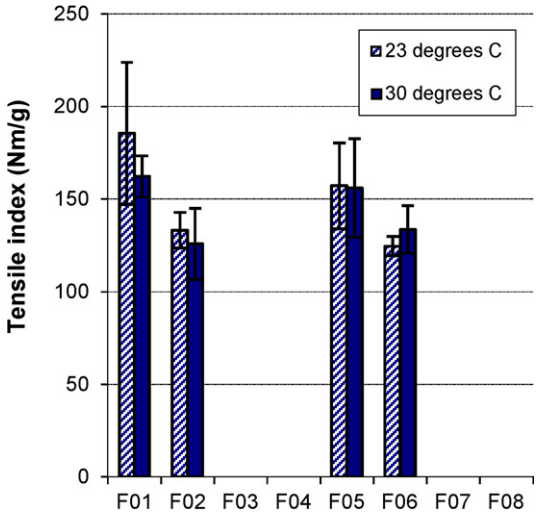

Fig. 1. Tensile index of films made of cellulose nanofibrils.

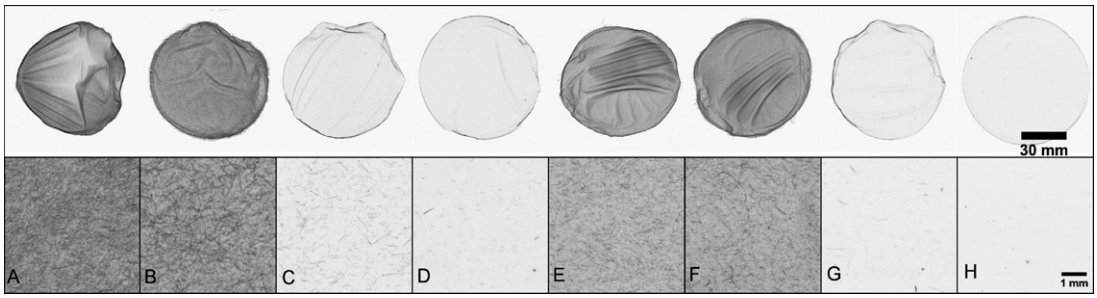

Fig. 2. Properties of nanofibril-based films. (A)–H) correspond to the series F01–F08, respectively. (Upper row) Images were acquired at 300 DPI for shrinkage analysis. (Lower row) Images acquired at 2400 DPI applied for transparency analysis.

series. The differences with respect to the shrinkage degrees were presumptively related to the dimensions and composition of the produced fibrillated material, after homogenization.

To shed more light on this observation, scanner images of local areas were acquired with a resolution of 2400 DPI. The images reveal that the less treated samples (e.g. F01) contained a major fraction of pulp fibres that were partially fibrillated. The shrinkage was thus most probably caused by a global deformation induced by local cross-sectional shrinkages of the poorly fibrillated fibres. The *Eucalyptus* fibres (in e.g. samples F01 and F03) have a larger fraction of hemicellulose. Hemicellulose swells easily and may thus have caused the dimensional instability during drying. It is also worth to notice that the oxidized sample F08 had less shrinkage. The F08 film appeared homogeneous with a low content of fibre fragments.

The transmittances of the films were evaluated in the digital images acquired at 2400 DPI. Based on a stable reproduction of greylevels of an IT8 target (Fig. 3 right), the scanner approach was considered appropriate for assessing the transparencies of the films. In addition, the scanner analysis proposed in this study yields a direct quantification of the transparency levels of the films and visualization of the unfibrillated material, compared to indirect methods such as spectrometers, applied to verify the degree of fibrillation (see e.g. Iwamoto et al., 2008). The transmittance levels of the films F01, F02, F05 and F06 (23 and 30 °C) are significant lower than the TEMPO pre-treated samples (Fig. 3, right). TEMPO pre-treated samples had a minor fraction of fibres. It is worth to notice that the series of films dried at 30 °C showed lower transparency values due to some opaque areas caused by bubbles. A temperature of 30 °C might have induced a relatively fast drying of the films. The films consolidated faster, limiting a homogeneous redistribution of the nanofibrillated material. A significant negative effect of the drying factor was thus detected. Films made of *Eucalyptus* fibrillated material yielded generally lower transparency levels, which may be related to a lower fibrillation of the *Eucalyptus* fibres. However, based on a statistical analysis of the factorial experiment it appears that the presumptive effect of the fibre factor is not significant. Hence, irrespective of the fibre type, the fibres and fibre fragments presumptively form a network of pores, which are sufficiently large for scattering light (roughly > 0.2 μm) (Alince, Porubska, & Van De Ven, 2002). The pores increase the light scattering potential of the material, increasing also the opacity, which reduces the corresponding transparency levels.

3.4. Assessment of surface structures

A surface assessment at the nanoscale was performed with AFM (Fig. 4). The results evidence that the surface structures are not only affected by the unfibrillated fibres (Fig. 2), but is also affected by a differential morphology of the produced nanofibrils. The surface structures assessed at sub-micron wavelengths reveals thus large differences between the untreated and TEMPO pre-treated samples (Fig. 4, right). The F03 and F04 (TEMPO pre-treated) are smoother (lower Sq) than the F01 and F02 samples, which were not TEMPO pre-treated. Contrary to the samples F01 and F02, the TEMPO pre-treated samples (F03, F04) are composed of nanofibrils having relatively homogeneous diameters (Fig. 4, left).

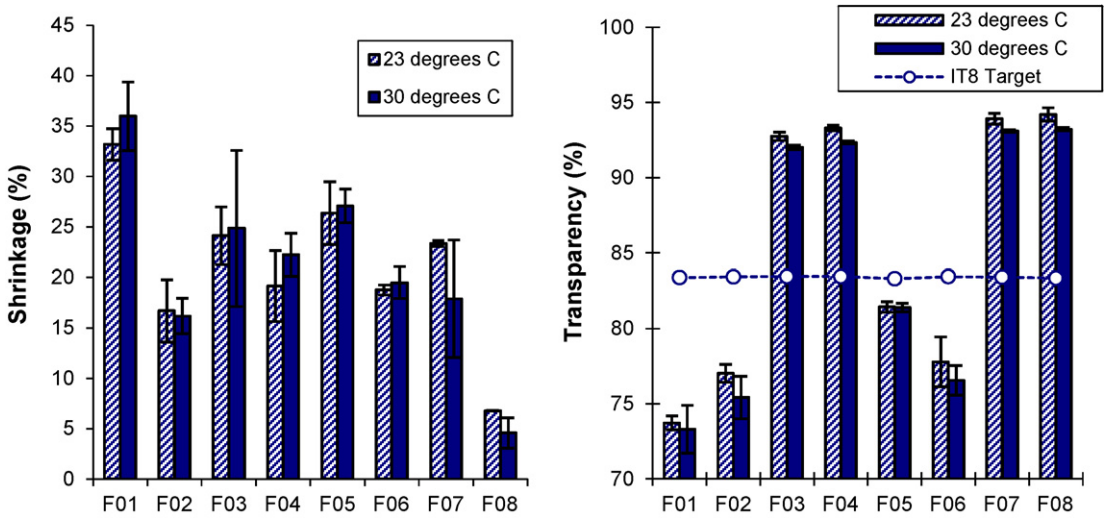

Fig. 3. Shrinkage (left) and transparency (right) levels of films F01–F08 (Table 1). The transparency levels of a field in a IT8 target are included for verification of the stability of the scanner during image acquisition.

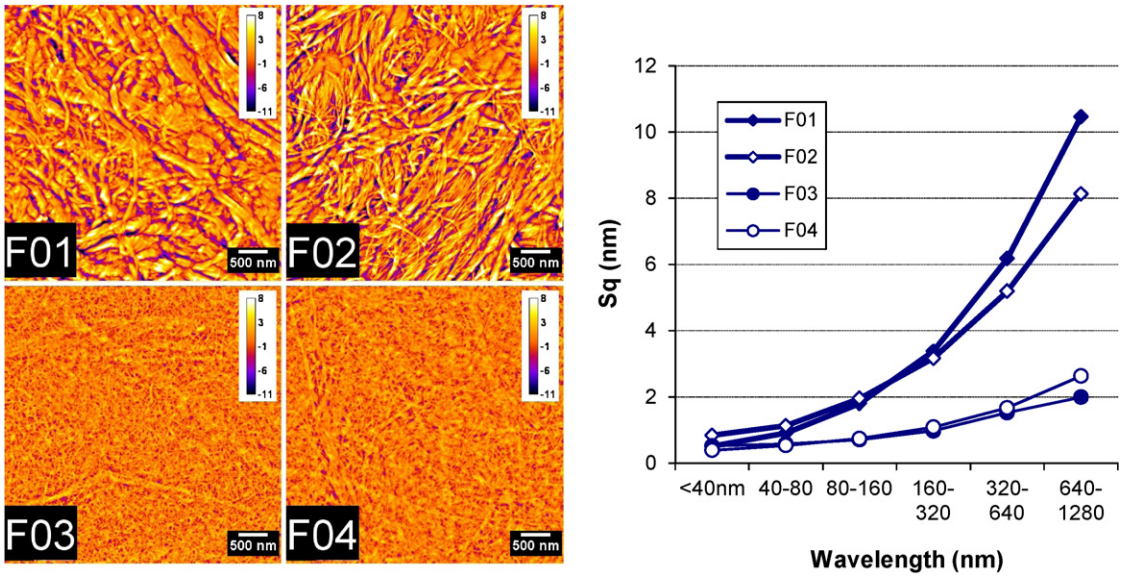

Fig. 4. (Left) Surface roughness (Sq) of samples F01–F04. The images have been filtered to better visualize the nanofibrils. The scale (bar = 500 nm) and calibration (height between 8 and −11 nm) bars are given. (Right) Surface roughness as a function of wavelength. The wavelength in the *x*-axis indicates the structure scales (lateral scales) that were assessed in the estimation of the roughness.

3.5. Energy consumption

From an industrial point of view, the energy requirements for producing a given nanofibril quality is most interesting. The results presented in this study have given clear indications of the effect TEMPO has on the applied pulp fibres. With the applied consistency (0.5%) and the applied pressure (1000 bar), the accumulated energy consumption is high, i.e. roughly 10,000 kWh/t per pass through the homogenisator However, for the same number of passes, TEMPO pre-treatment facilitates the fibrillation and thus reduces the number of unfibrillated fibres (Fig. 2).

Several homogenization processes were performed as an attempt to shed more light on the energy consumption, which is required to produce a given nanofibrillated material. Fig. 5 shows a considerable reduction in energy consumption when homogenizing with 200 and 600 bar pressure, while the reduction in the transparency levels are only slightly affected. Depending on the application area, Fig. 5 suggests that it is possible to design a given procedure for producing nanofibrils with a given morphology and utilizing acceptable energy levels. Keep in mind that increasing the concentration will reduce the energy consumption considerably.

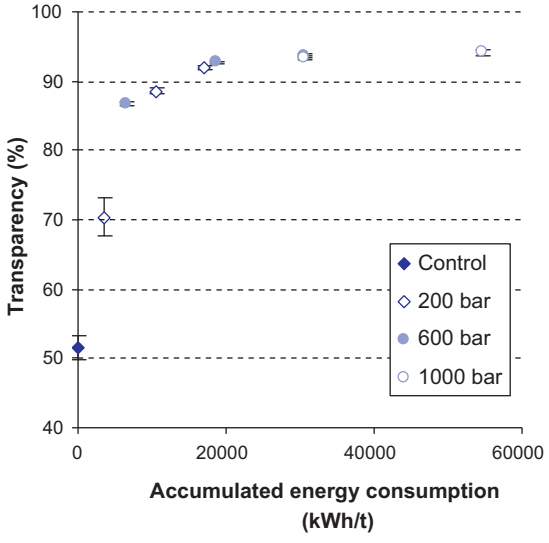

Fig. 5. Transparency levels of films as a function of pressure utilized during the homogenization of *P. radiata* pulp fibres, pre-treated with TEMPO. The control sample corresponds to films made of *P. radiata* pulp fibres, which were not homogenized.

The major effect of the TEMPO pre-treatment is on the facilitation of the fibrillation of the fibres. The results indicate that *P. radiata* is more susceptible to be fibrillated than *Eucalyptus*, although *P. radiata* contains less hemicellulose and has a lower amount of charged groups per unit mass after TEMPO pre-treatment.

The low fibrillation degree of *Eucalyptus*, compared to *P. radiata*, may also have been influenced by the high content and location of xylan in the hardwood fibres (Table 2). Xylan does not have the C6 in which the selective oxidation takes place when using TEMPO as a catalyst. This is confirmed in Table 2, where it is reported that the xylan content is not significantly affected by the TEMPO-mediated oxidation. Xylan has been reported to be mostly located in the outer layers of the secondary wall due to sorption phenomena during kraft pulping (Ylnner & Enström, 1956, 1957). It seems that xylan from hardwood is more easily reallocated in cellulose surfaces compared to xylan from softwood (Hansson & Hartler, 1969). This may suggests that the outer layers of the *Eucalyptus* fibre wall had a minor oxidation during the TEMPO pre-treatment, compared to *P. radiata*. *Eucalyptus* may thus have a fraction of poorly oxidized outer layers, which does not fibrillate easily during homogenization, thus presumptively protecting the interior fibre wall structure.

4. Conclusions

Nanofibrils were produced from the softwood and hard wood pulp fibres. A detailed comparison was performed considering (i) the chemical composition of the pulp fibres and (ii) the properties of the produced nanofibrillated material. TEMPO pre-treatment had a major effect on the fibrillation of the pulp fibres. Irrespective of the fibre type, once fibrillated, the produced nanofibrils seem to have no differences with respect to their morphology, as revealed by AFM analysis. For a given number of passes through the homogenizator (same energy consumption), samples pre-treated with TEMPO are more homogeneously fibrillated, which have a major effect on their

corresponding structural and performance properties. Model films made of *Pinus radiata* nanofibrils evidenced less shrinkage and had a larger light transmittance level than the corresponding *Eucalyptus*-based nanofibril films.

Acknowledgements

We applied the "sequence-determines-credit" (SDC) approach for the sequence of authors. Ingebjørg Leirset and Mirjana Filipovic (PFI AS) are grateful acknowledged for good cooperation during the performance of this work. The authors thank Raúl González Murillo (Research and development manager, CMPC Celulosa S.A., Chile) for providing the market pulps applied in this study and necessary information. The work was financed by the Research Council of Norway through the grant 193706/S50. Pedro G. Toledo (Universidad de Concepción) thanks Fondecyt 1090781.

References

Alince, B., Porubska, J., & Van De Ven, T. G. M. J. (2002). Light scattering and microporosity in paper. *Journal of Pulp and Paper Science*, *28*(3), 93–98.

Aulin, C., Gällstedt, M., & Lindström, T. (2010). Oxygen and oil barrier properties of microfibrillated cellulose films and coatings. *Cellulose*, *17*, 559–574.

Cao, B., Tschirner, U., Ramaswamy, S., & Webb, A. (1997). A Rapid modified gas chromatographic method for carbohydrate analysis of wood pulps. *TAPPI Journal*, *80*(9), 193–197.

Chinga, G., Johnsen, P. O., Dougherty, R., Lunden-Berli, E., & Walter, J. (2007). Quantification of the 3D microstructure of SC surfaces. *Journal of Microscopy*, *227*(3), 254–265.

Chinga-Carrasco, G., & Syverud, K. (2010). Computer-assisted quantification of the multi-scale structure of films made of nanofibrillated cellulose. *Journal of Nanoparticle Research*, *12*(3), 841–851.

Dexter, R. J. (1993). Field uses of scanning dirt counter technology. *Program Paper Recycling*, *2*(4), 40–45.

Eriksen, Ø., Syverud, K., & Gregersen, Ø. (2008). The use of microfibrillated cellulose produced from kraft pulp as a strength enhancer in TMP paper. *Nordic Pulp Paper Research Journal*, *23*(3), 299–304.

Fukuzumi, H., Saito, T., Iwata, T., Kumamoto, Y., & Isogai, A. (2009). Transparent and high gas barrier films of cellulose nanofibers prepared by TEMPO-mediated oxidation. *Biomacromolecules*, *10*, 162–165.

Habibi, Y., Chanzy, H., & Vignon, M. R. (2006). TEMPO-mediated surface oxidation of cellulose whiskers. *Cellulose*, *13*, 679–687.

Hansson, J., & Hartler, N. (1969). Sorption of Hemicelluloses on Cellulose Fibres. *Svensk Papperstidning*, *72*, 521–530.

Heijnes-Son-Hultén, A. (2007). *Method for preparing microfibrillar polysaccharide*. Patent no. WO 2007/001229 A1.

Henriksson, M., & Berglund, L. A. (2007). Structure and properties of cellulose nanocomposite films containing melamine formaldehyde. *Journal of Applied Polymer Science*, *106*, 2817–2824.

Hult, E.-L., Iotti, M., & Lenes, M. (2010). Efficient approach to high barrier packaging using microfibrillar cellulose and shellac. *Cellulose*, *17*, 575–586.

Iwamoto, S., Abe, K., & Yano, H. (2008). The effect of hemicelluloses on wood pulp nanofibrillation and nanofiber network characteristics. *Biomacromolecules*, *9*, 1022–1026.

Klemm, D., Schumann, D., Kramer, F., Hessler, N., Hornung, M., Schmauder, H.-P., et al. (2006). Nanocelluloses as innovative polymers in research and application. *Advances in Polymer Science*, *205*, 49–96.

Minelli, M., Baschetti, M. G., Doghieri, F., Ankerfors, M., Lindström, T., Siró, I., et al. (2010). Investigation of mass transport properties of microfibrillated cellulose (MFC) films. *Journal of Membrane Science*, *358*, 67–75.

Mörseburg, K., & Chinga-Carrasco, G. (2009). Assessing the combined benefits of clay and nanofibrillated cellulose in layered TMP-based sheets. *Cellulose*, *16*(5), 795–806.

Pääkkö, M., Ankefors, M., Kosonen, H., Nykänen, A., Ahola, S., Österberg, M., et al. (2007). Enzymatic hydrolysis combined with mechanical shearing and high-pressure homogenization for nanoscale cellulose fibrils and strong gels. *Biomacromolecules*, *8*, 1934–1941.

Saito, T., & Isogai, A. (2004). TEMPO-mediated oxidation of native cellulose. The effect of oxidation conditions on chemical and crystal structures of the water-insoluble fractions. *Biomacromolecules*, *5*, 1983–1989.

Saito, T., Nishiyama, Y., Putaux, J. L., Vignon, M., & Isogai, A. (2006). Homogeneous suspensions of individualized microfibrils from TEMPO-catalyzed oxidation of native cellulose. *Biomacromolecules*, *7*(6), 1687–1691.

Saito, T., Kimura, S., Nishiyama, Y., & Iasogai, A. (2007). Cellulose nanofibers prepared by TEMPO-mediatedoxidation of native cellulose. *Biomacromolecules*, *8*, 2485–2491.

Sihtola, H., Kyrklund, B., Laamanen, L., & Palenius, I. (1963). Comparison and conversion of viscosity and DP-values determined by different methods. *Paperi ja Puu*, *4a*, 225–232.

Stelte, W., & Sanadi, A. R. (2009). Preparation and characterization of cellulose nanofibers from two commercial hardwood and softwood pulps. *Industrial & Engineering Chemistry Research*, *48*, 11211–11219.

Syverud, K., & Stenius, P. (2009). Strength and permeability of MFC films. *Cellulose*, *16*(1), 75–85.

Syverud, K., Xhanari, K., Chinga-Carrasco, G., Yu, Y., & Stenius, P. (2010). Films made of cellulose nanofibrils-surface modification by adsorption of a cationic surfactant and characterisation by computer-assisted electron microscopy. *Journal of Nanoparticle Research*, doi:10.1007/s11051-010-0077-1

Taniguchi, T., & Okamura, K. (1998). New films produced from microfibrillated natural fibres. *Polymer International*, *47*, 291–294.

Turbak, A. F., Snyder, F. W., & Sandberg, K. R. (1982). *Food products containing microfibrillated cellulose*. US Patent no. 4,341,807, Jul. 27.

Turbak, A. F., Snyder, F. W., & Sandberg, K. R. (1983). Microfibrillated cellulose, a new cellulose product: properties, uses, and commercial potential. *Journal of Applied Polymer Science*, *37*, 815–827.

Turbak, A. F., Snyder, F. W., & Sandberg, K. R. (1985). *Suspensions containing microfibrillated cellulose*. US Patent no. 4,500,546, February 19.

Ylnner, S., & Enström, B. (1956). Studies of the adsorption of xylan on cellulose fibre during the sulphate cook – Part 1. *Svensk Papperstidning*, *59*, 229–232.

Ylnner, S., & Enström, B. (1957). Studies of the adsorption of xylan on cellulose fibre during the sulphate cook – Part 2. *Svensk Papperstidning*, *60*, 549–554.

Zimmermann, T., Bordeanu, N., & Strub, E. (2010). Properties of nanofibrillated cellulose from different raw materials and its reinforcement potential. *Carbohydrate Polymers*, *79*(4), 1086–1093.